

## Viscoelastic Properties of Dilute Aqueous Solution of Methylcellulose at Ultrasonic Frequencies

TAKESHI AMARI and MATAO NAKAMURA, *Institute of Industrial Science, University of Tokyo, Tokyo, Japan*

### Synopsis

The viscoelastic properties of dilute aqueous solutions of methylcellulose at ultrasonic frequencies were investigated by a torsional method using quartz crystal resonators. The concentration dependences of  $G'$  and  $G'' - \omega\eta_s$  increased with increasing temperature at 13 kHz, but at higher frequencies  $G'$  and  $G'' - \omega\eta_s$  were simply proportional to the concentration irrespective of temperature. These results may be explained by the difference of corresponding viscoelastic mechanism at measuring frequencies. In order to examine the configuration of methylcellulose in water, which changes remarkably with temperature, the intrinsic values at various temperatures were experimentally obtained by extrapolation to zero concentration, and the frequency dependence of intrinsic dynamic viscosity was examined. The values of components of the complex intrinsic viscosity at various temperatures and their frequency dependences were quantitatively compared with those calculated from the Tschoegl theory. The values of hydrodynamic strength parameter in the Tschoegl theory for an aqueous solution of methylcellulose increased with increasing temperature, and an effect of the internal viscosity due to the aggregation of methylcellulose was observed at higher temperatures. However, on the whole, the viscoelastic behavior was relatively close to Rouse-like behavior.

### INTRODUCTION

Viscoelastic properties of dilute polymer solutions have been investigated mainly in the region of ultrasonic frequencies, and various techniques have been developed for the measurements in this region. Among them, the torsional method using a crystal resonator is most frequently adopted. As the resonator having evaporated electrodes should be fully dipped in a measuring solution, this method has been usually applied to polymer solutions that are not electrical conductors. In order to apply this method to an aqueous polymer solution, modified resonators were used in this study. Furthermore, we constructed two new types of resonators such as a huge quartz crystal resonator and a jointed resonator and used them to cover a wide range of frequency.

In previous reports,<sup>1,2</sup> we have found that the viscoelastic properties of an aqueous solution of methylcellulose greatly depend on the peculiar behavior of methylcellulose in water. Namely, at lower temperatures the molecular chains of methylcellulose are fully hydrated due to the decreased mobility of the molecules, and consequently the probability of contacting

molecular chains with each other is low. The polymer molecule in solution is thus prevented from contact with other polymers, and aggregation does not occur. However, as the temperature increases, water molecules adsorbed on methylcellulose are gradually released, and the natural tendency for methylcellulose molecules to interact with each other becomes predominant, and aggregation occurs. In the concentrated solution of methylcellulose, this temperature-dependent intermolecular interaction was investigated from various viscoelastic properties such as the entanglement density of structural networks in solution, the modulus of the entanglement networks, and the relation between recoverable shear and shear stress. However, in dilute aqueous solutions, this effect was not investigated satisfactorily from the viewpoint of viscoelastic properties. Therefore, in the present study, the viscoelastic properties were measured by a torsional method using quartz crystal resonators in the region of ultrasonic frequencies, in order to investigate the relation between viscoelastic properties and temperature-dependent intermolecular interactions of methylcellulose at dilute aqueous solutions at various temperatures. Moreover, we attempted to clarify the configuration of isolated methylcellulose chains in water at various temperatures.

## EXPERIMENTAL

### Quartz Crystal Resonator

The measurements of viscoelastic properties were carried out by the torsional method as described by Masson et al.<sup>3,4</sup> and Wada et al.<sup>5</sup> The quartz crystal was cut with its length along the *x*-axis and supported by four phosphor bronze wires. Each wire formed the electrical connection to one of four quadrantal electrodes of evaporated gold which ran the length of the crystal resonator. In this study, the electrodes were evaporated only on the upper half of the resonator in order to measure the viscoelastic properties of electrically conductive liquids. The resonator was moved vertically by means of a micrometer screw, and the lower fourth of the resonator was dipped into the solution. The level of the solution was at the lower nodal plane of the resonator so that errors due to the variation of the level of the solution and effect of the surface tension of the solution might be minimized.

Electrodes were not affected by the temperature of sample solutions under the condition in this study. In our method, it was necessary to use the double length resonator in order to measure at the same frequency range as in the conventional method with the same degree of precision, and the resonator used at the lowest frequency was 150 mm in length. As it is generally difficult to obtain such a huge monocrystal resonator, we devised a jointed crystal resonator as a substitute for the huge monocrystal resonator. The adhesive phase of jointed crystal resonator should be a loop of the torsional vibration. An epoxy-type adhesive was used to adhere the crys-

details to each other, which does not interfere with measurements. More details of the jointed resonators have been described elsewhere.<sup>6,7</sup> As the crystal resonators were supported by wires at the midpoint of the electrodes evaporated on the upper half of the crystal, the second harmonic of torsional vibration was mostly used. Moreover, the first and sixth harmonics were also used to extend the measurable frequency range.

The crystal resonator and the modes of torsional vibration are schematically shown in Figure 1. The conductance curves of the huge crystal resonator in toluene at 25°C at various modes are shown in Figure 2. The resonance width of the second mode is smaller than those of other modes, and the conductance of the second mode at resonant frequency is largest. Therefore, the second harmonics were mostly used. The band width

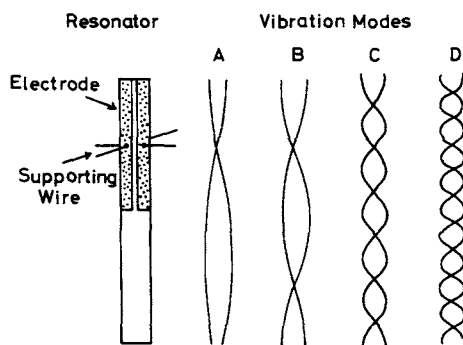


Fig. 1. Schematic diagram of crystal resonator and vibration modes: (A) first mode; (B) second mode; (C) sixth mode; (D) tenth mode.

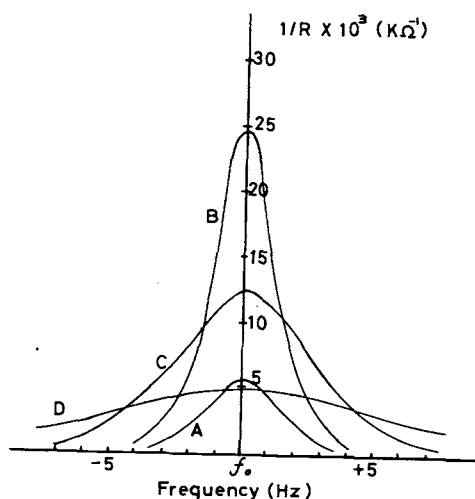


Fig. 2. Conductance vs. frequency for a huge crystal resonator in toluene at 25°C at various vibration modes: (A) first mode; (B) second mode; (C) sixth mode; (D) tenth mode.

$(\Delta f)_{1/2}$  is 2.4 Hz at the first mode, 2.0 Hz at the second, 3.8 Hz at the sixth, and 7.4 Hz at the tenth, respectively. The value of the equivalent electrical inductance ( $L_c$ ) at each harmonics was calculated according to the procedure by Rouse and Sittle.<sup>8</sup> The value of  $L_c$  at the first mode is larger than the other, namely, 6897 H at the first, 2378 H at the second, 2389 H at the sixth, and 2390 H at the tenth mode. In a conventional resonator, the values of electromechanical constants  $K_1$  and  $K_2$  can be calculated from the dimensions and piezoelectric constants of the crystal. However, for the resonators used in this study, these values had to be experimentally determined using a Newtonian liquid. Calibration was carried out for each crystal at each harmonic using ethylene glycol. The constants of these crystal resonators are given in Table I. On the whole, the values of the equivalent electrical resistance of the crystal  $R_0$  and the electromechanical constant  $K_1$  at the first and sixth harmonics are larger than those at the second harmonic. Accordingly, the precision of the latter is higher than that of the former. However, it is interesting that the value of  $K_1$  at the sixth harmonic for a huge crystal resonator is smaller than that at the second harmonic for a jointed one. Electrodes were protected by 2% silicon oil in toluene in order to prevent the interferences of moisture.

### Principles of Measurement

According to Rouse and Sittle,<sup>8</sup> the values of the mechanical resistance  $R_M$  and reactance  $X_M$  for each crystal at each harmonic may be written as follows:

$$R_M = (\pi f \rho \eta_s)^{1/2} + [(R_p - R_s)/K_1] \quad (1)$$

$$X_M = (\pi f \rho \eta_s)^{1/2} + [(f_s - f_p)/K_2] + C \quad (2)$$

where  $f$  is frequency of applied shear stress;  $\eta_s$  is the viscosity of solvent;  $\rho$  is density of solution;  $R_s$  and  $R_p$  are electrical resistances of crystal in solvent and solution, respectively;  $f_s$  and  $f_p$  are resonant frequencies of crystal in solvent and solution, respectively, and  $C$  is an empirical correction term due to the roughness of the surface of crystal. As already reported,<sup>6,7</sup> these equations can also be applied to our arrangements. The values of  $G'$  and  $G''$  (components of complex rigidity) and  $\eta'$  (dynamic viscosity) were related to the components of the mechanical impedance,  $R_M$  and  $X_M$ , by the following equations:

$$G' = (R_M^2 - X_M^2)/\rho \quad (3)$$

$$G'' = 2R_M X_M/\rho \quad (4)$$

$$\eta' = 2R_M X_M/\rho \omega \quad (5)$$

where  $\omega$  is an angular frequency of applied shear stress.

Values of electrical impedance of crystal resonator in liquid were measured with a phase-sensitive detector designed by Torikai and Negishi.<sup>9</sup> The phase characteristics of the detector become uncertain in the frequency

TABLE I  
 Constants of Crystal Resonators

Resonator	Length, mm	Diameter, mm	Electrode, mm	Modes	$f_0^a$ , kHz	$R_0^a$ , k $\Omega$	$L_c \times 10^{-10}$ , H	$K_1 \times 10^{-3b}$	$K_2^b$
Mono crystal	150	10	75	1st	13.0649	71.4	6.897	10.25	0.130
				2nd	26.1450	6.89	2.378	2.045	0.194
	50	5	25	6th	78.5761	8.85	2.389	2.145	0.269
				2nd	78.9130	20.2	1.065	1.201	0.370
Jointed crystal	100	5	50	2nd	131.085	8.7	0.7018	0.908	0.530
				2nd	39.3162	5.15	2.490	2.747	0.279
	100	5	25	6th	117.846	9.34	2.294	3.659	0.356
				2nd	78.7560 <sup>c</sup>	12.0	2.854	2.280 <sup>c</sup>	0.263 <sup>c</sup>

<sup>a</sup> Measured at 25°C.

<sup>b</sup> Calculated from the measured values of ethylene glycol.

<sup>c</sup> The level of the solution was at the lowest nodal plane of the resonator.

range above 100 kHz, so that corrections of the electronic circuit were necessary. The value of the resonant frequency shift was measured with electronic counter. The values of  $G'$ ,  $G''$ , and  $\eta'$  were measured at frequencies of 13, 26, 39, 78, and 117 kHz using resonators listed in Table I. The measurements at 78 kHz were carried out using only the monocrystal resonator, which was 50 mm in length. The room temperature was controlled at  $25.0 \pm 0.1^\circ\text{C}$  in order to prevent experimental errors due to the variation of crystal constants. The temperatures of sample solutions were controlled to an accuracy of  $\pm 0.01^\circ\text{C}$  by a water jacket where water of constant temperature was circulated. The experimental error was within 1% for the solution with viscosity of 0.01 poise.

### Steady Shear Viscosity

Viscosity measurements were carried out in a temperature-controlled bath. The steady-shear viscosities of sample solutions were measured at  $10^\circ$ ,  $25^\circ$ , and  $40^\circ \pm 0.01^\circ\text{C}$  using an Ostwald viscometer. The efflux times of the solutions (typically about 240 sec) were reproducible to  $\pm 0.1$  sec. The kinetic energy correction was neglected because it was very small under all experimental conditions.

### Samples

The same commercial product of methylcellulose ( $\bar{M}_w = 1.10 \times 10^5$ , methoxyl content 29.5%) as previously reported<sup>1,2</sup> was mainly used.

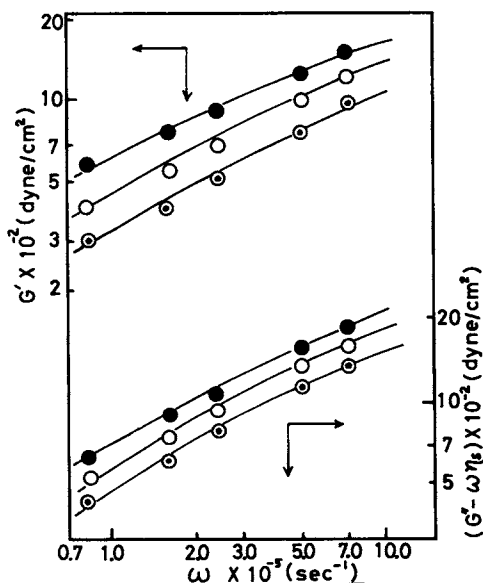


Fig. 3. Frequency dependence of  $G'$  and  $G'' - \omega\eta_s$  for a 0.002 g/ml aqueous solution of methylcellulose: (●) measured at  $10^\circ\text{C}$ ; (○) measured at  $25^\circ\text{C}$ ; (◐) measured at  $40^\circ\text{C}$ .

Moreover, methylcellulose samples of different molecular weights were used in order to calculate a non-Gaussian parameter in the Tschoegl theory<sup>10,11</sup> and their molecular weights were  $4.10 \times 10^4$ ,  $6.30 \times 10^4$ , and  $8.60 \times 10^4$ , respectively. All measurements were carried out in concentrations ranging from 0.0005 g/ml to 0.002 g/ml, at temperatures of 10°, 25°, and 40°C.

Since the presence of sodium chloride influences the effective electric resistance of crystal resonators in dilute aqueous polymer solution, the samples were washed with methanol using a Soxhlet extractor for 10 hr, to completely remove sodium chloride remaining in the samples.

## RESULTS AND DISCUSSION

### Viscoelastic Properties at Finite Concentrations

The frequency dependences of  $G'$  and  $G'' - \omega\eta_s$  for aqueous solutions of methylcellulose at concentrations of 0.002 and 0.0005 g/ml at various temperatures are shown in Figures 3 and 4. Figure 3 shows the results at a concentration of 0.002 g/ml, and both  $G'$  and  $G'' - \omega\eta_s$  at each temperature are roughly proportional to  $\omega^{1/2}$ . The temperature dependence of  $G'$  is more remarkable than that of  $G'' - \omega\eta_s$ . The ratio  $(G'' - \omega\eta_s)/G'$  is 1.05 at 10°C, 1.27 at 25°C, and 1.60 at 40°C. At a concentration of 0.0005 g/ml (Fig. 4), at 10°C,  $G'$  and  $G'' - \omega\eta_s$  show similar frequency dependences as observed for 0.002 g/ml, whereas at 40°C,  $G'$  and  $G'' - \omega\eta_s$  are roughly proportional to  $\omega$  and  $\omega^{2/3}$ , respectively. The temperature de-

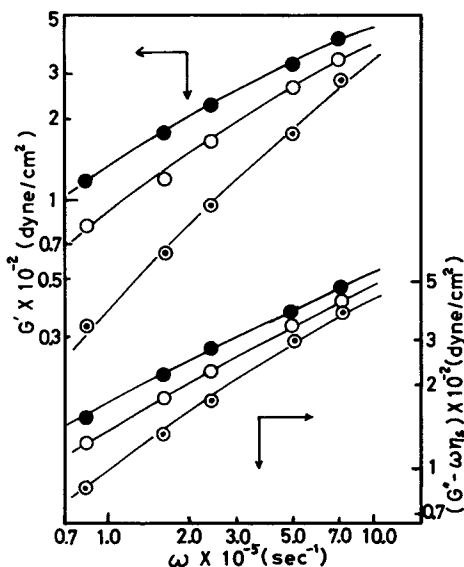


Fig. 4. Frequency dependence of  $G'$  and  $G'' - \omega\eta_s$  for a 0.0005 g/ml aqueous solution of methylcellulose: (●) measured at 10°C; (○) measured at 25°C; (⊙) measured at 40°C.

pendences of  $G'$  and  $G'' - \omega\eta_s$  at a concentration of 0.0005 g/ml are larger than those at a concentration of 0.002 g/ml.

From these results, it is concluded that the time-temperature superposition principle is not applicable to this system, and it is supposed that the corresponding viscoelastic mechanism varies with temperature. The concentration dependences of  $G'$  and  $G'' - \omega\eta_s$  are shown in Figures 5, 6, and 7 for 13 kHz, 39 kHz, and 117 kHz, respectively. Previously we have reported that at lower frequencies, the concentration dependence of  $G'$  is more remarkable and becomes larger with increasing temperature in a concentration range of 0.007 to 0.03 g/ml, and this phenomenon can be explained by intermolecular interactions. At 13 kHz,  $G'$  increases with increasing concentration more rapidly than those at other frequencies and the concentration dependence of  $G'$  becomes larger with increasing temperature. Namely, the values of  $G'$  are proportional to  $c^{1.1}$  at 10°C,  $c^{1.3}$  at 25°C, and  $c^{1.6}$  at 40°C, where  $c$  is the polymer concentration. This tendency agrees well with that at lower frequencies. However, the corresponding viscoelastic mechanisms at ultrasonic frequencies at very low concentra-

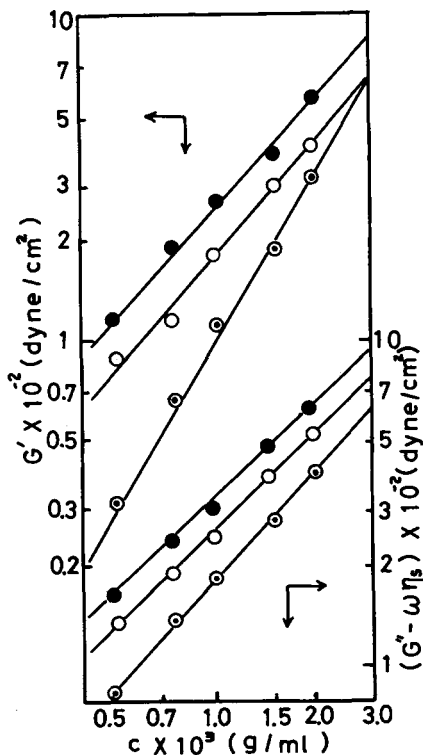


Fig. 5. Concentration dependence of  $G'$  and  $G'' - \omega\eta_s$  at 13 kHz for aqueous solution of methylcellulose: (●) measured at 10°C; (○) measured at 25°C; (⊙) measured at 40°C.



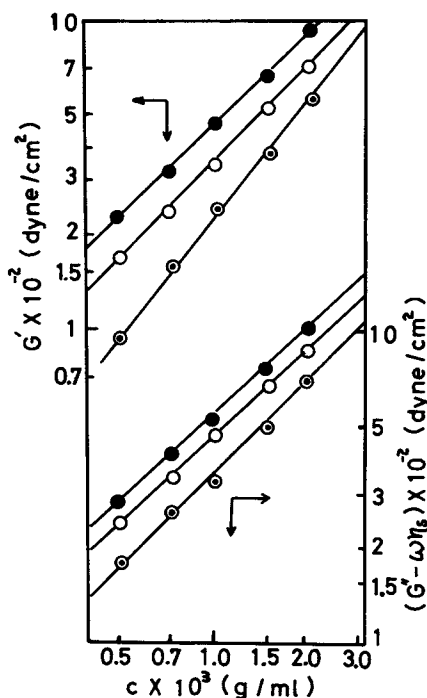


Fig. 6. Concentration dependence of  $G'$  and  $G'' - \omega\eta_s$  at 39 kHz for aqueous solution of methylcellulose: (●) measured at 10°C; (○) measured at 25°C; (⊙) measured at 40°C.

tions differ from those at low frequencies at relatively high concentrations which mainly depend on the entanglement couplings of molecular chains.

On the other hand, at higher frequencies, the concentration dependence of viscoelastic properties for an aqueous solution of methylcellulose decreases, and the same tendency is observed irrespective of temperature. Above 100 kHz, the values of  $G'$  and  $G'' - \omega\eta_s$  are proportional to  $c$  and their temperature dependences become indefinite. These results may be explained by the difference of corresponding viscoelastic mechanism at measuring frequencies.

### Intrinsic Viscoelastic Properties

In Figure 8, reduced viscosity  $\eta_{sp}/c$  is plotted against  $c$  for aqueous solutions of methylcellulose at various temperatures. The relation between  $\eta_{sp}/c$  and concentration is nonlinear at each temperature. Therefore, the intrinsic viscosity  $[\eta]$  for these solutions cannot be obtained by extrapolation to zero concentration. The Huggins equation is applicable only in quite dilute solutions in which the value of relative viscosity  $\eta/\eta_s$  is smaller than 2.0. In the aqueous solutions of methylcellulose used in this study, the value of the relative viscosity was larger than 2.0 even at a concentration of 0.001 g/ml. This phenomenon suggests that for an aqueous solution of

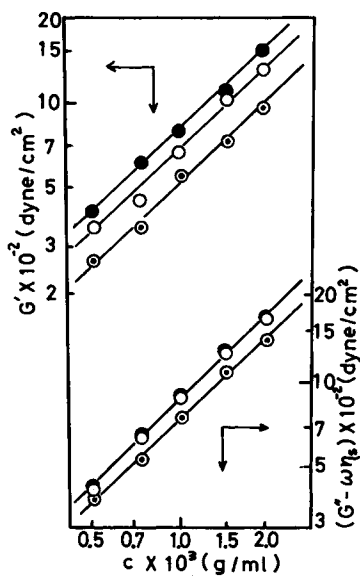


Fig. 7. Concentration dependence of  $G'$  and  $G'' - \omega\eta_s$  at 117 kHz for aqueous solution of methylcellulose: (●) measured at 10°C; (○) measured at 25°C; (⊙) measured at 40°C.

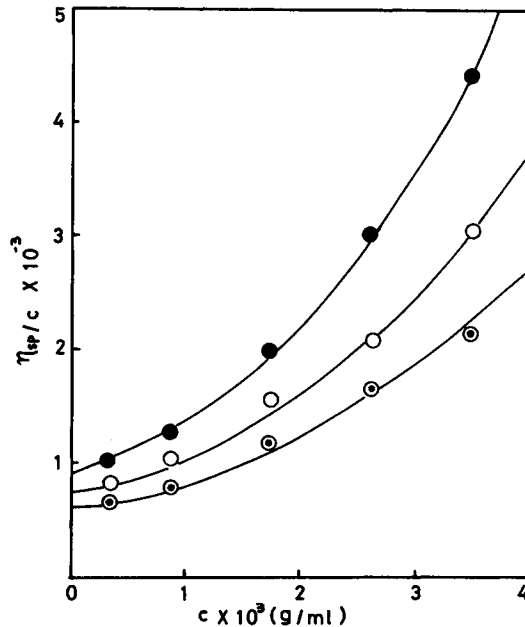


Fig. 8. Plot of  $\eta_{sp}/c$  vs.  $c$  for aqueous solution of methylcellulose: (●) measured at 10°C; (○) measured at 25°C; (⊙) measured at 40°C.

methylcellulose, the intermolecular interaction cannot be neglected even in very dilute solution. According to Martin,<sup>12,13</sup> the following relations apply over a wide range of concentration:

$$\eta_{sp}/c = [\eta] \exp(k'[\eta]c), \quad (6)$$

$$\ln(\eta_{sp}/c) = \ln[\eta] + k'[\eta]c \quad (7)$$

where  $k'$  is an empirical constant.

For the above solutions, the relations between  $\ln(\eta_{sp}/c)$  and  $c$  are shown in Figure 9. In this figure,  $\ln(\eta_{sp}/c)$  is approximately a linear function of  $c$  up to the highest concentration investigated, and the intrinsic viscosity for each solution can be calculated from the intercept of each straight line;  $[\eta]$  is 845 ml/g at 10°C, 706 ml/g at 25°C, and 578 ml/g at 40°C. The intrinsic viscosity decreases with increasing temperature in an aqueous solution of methylcellulose.

Generally, it is necessary to extrapolate to infinite dilution in order to investigate the viscoelastic properties and the configuration of an isolated polymer molecule. The complex intrinsic viscosity for oscillatory flow is defined as follows:

$$[\eta^*] = [\eta'] - i[\eta''] \quad (8)$$

$$= \lim_{c \rightarrow 0} (\eta^* - \eta_s)/\eta_s c \quad (9)$$

where  $\eta^* = \eta' - i\eta''$  is the complex viscosity at a finite concentration.

In the present study, in aqueous solutions of methylcellulose at various temperatures,  $[\eta']$  and  $[\eta'']$  were obtained in order to investigate the relation between temperature and configuration of polymer chains. In Figure 10,  $(\eta' - \eta_s)/c\eta_s$  is plotted versus  $c$  for aqueous solutions of methylcellulose at frequencies of 13 kHz, 39 kHz, and 117 kHz at various temperatures. The concentration dependence of  $(\eta' - \eta_s)/c\eta_s$  is smaller than that of  $\eta_{sp}/c$ . As

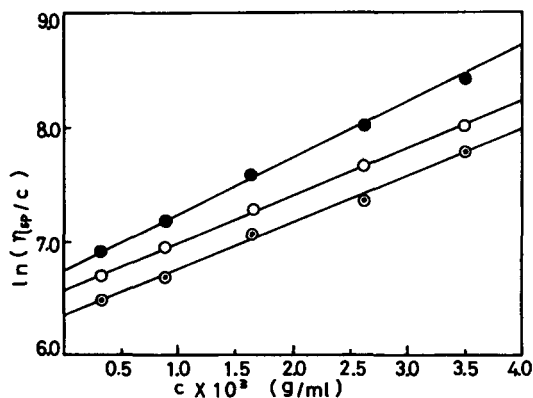


Fig. 9. Plot of  $\ln(\eta_{sp}/c)$  vs.  $c$  for aqueous solution of methylcellulose: (●) measured at 10°C; (○) measured at 25°C; (⊙) measured at 40°C.

expected from Figures 5, 6, and 7, the values of  $(\eta' - \eta_s)/c\eta_s$  are almost constant irrespective of concentrations, except for data at a frequency of 13 kHz at 25°C and 40°C. Although the plots of Figure 10 show some scattering, the intrinsic values can be obtained by extrapolation to zero concentration within an error of about 5%.

The frequency dependences of intrinsic dynamic viscosity  $[\eta']$  at various temperatures are shown in Figure 11. The value of  $[\eta]$  at 10°C is larger

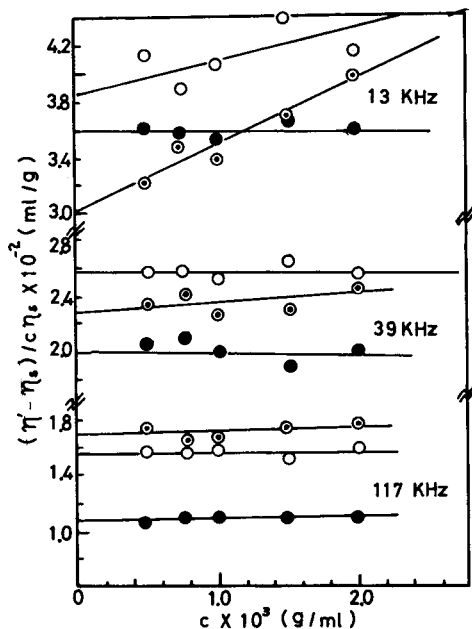


Fig. 10. Plot of  $(\eta' - \eta_s)/c\eta_s$  vs.  $c$  for aqueous solution of methylcellulose at frequencies of 13 kHz, 39 kHz, and 117 kHz: (●) measured at 10°C; (○) measured at 25°C; (◐) measured at 40°C.

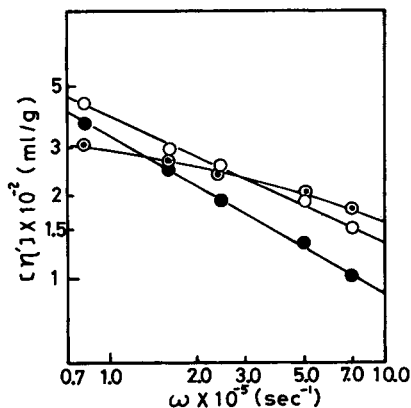


Fig. 11. Frequency dependence of  $[\eta']$  for aqueous solution of methylcellulose: (●) measured at 10°C; (○) measured at 25°C; (◐) measured at 40°C.

than that at any other temperature, while the values of  $[\eta']$  at  $10^\circ\text{C}$  are smaller than those at  $25^\circ\text{C}$ . The frequency dependence of  $[\eta']$  at  $10^\circ\text{C}$  is more remarkable than those at  $25^\circ\text{C}$  and  $40^\circ\text{C}$  over the frequency range investigated. The shape of the curve obtained at  $40^\circ\text{C}$  differs from those at  $10^\circ\text{C}$  and  $25^\circ\text{C}$ . As the frequency dependence of  $[\eta']$  at  $40^\circ\text{C}$  is smaller than those at  $10^\circ\text{C}$  and  $25^\circ\text{C}$ , at a frequency of 117 kHz the value of  $[\eta']$  at  $40^\circ\text{C}$ , which is the smallest at 13 kHz, is larger than those at  $10^\circ\text{C}$  and  $25^\circ\text{C}$ . This indicates that the configuration of polymer chains or the relaxation mechanism varies with temperature, and this phenomenon apparently depends on the peculiar aggregation process of the methylcellulose chains.

In order to investigate the temperature-dependent configuration of methylcellulose chain in more detail, the experimental results were compared quantitatively with the Tschoegl theory<sup>10,11</sup> for viscoelastic properties of polymer solution. In Figures 12, 13, and 14, the real and imaginary parts of the complex intrinsic viscosity which are normalized by the steady-flow intrinsic viscosity are plotted against normalized frequency  $\omega[\eta]\eta_s M/RT$ , which contains experimentally determined parameters only, where  $M$  is the molecular weight,  $R$  is the gas constant, and  $T$  is the absolute temperature. The non-Gaussian parameter of the Tschoegl theory,  $\epsilon$ , was calculated from the Stockmayer-Fixman plot<sup>14</sup> experimentally obtained according to the procedure of Tschoegl and co-workers.<sup>15,16</sup>

The Stockmayer-Fixman plots for aqueous solutions of methylcellulose at various temperatures are shown in Figure 15. The values of  $\epsilon$  were 0.085 at  $10^\circ\text{C}$ , 0.135 at  $25^\circ\text{C}$ , and 0.195 at  $40^\circ\text{C}$ . From this tendency, it is thought that an aggregation proceeds with increasing temperature and results in a deviation from the random coil hypothesis. In Figure 12, the experimental results at  $10^\circ\text{C}$  are shown together with the theoretical curves, which are calculated from the Tschoegl theory with  $\epsilon = 0.085$ ,  $h = 0$  and

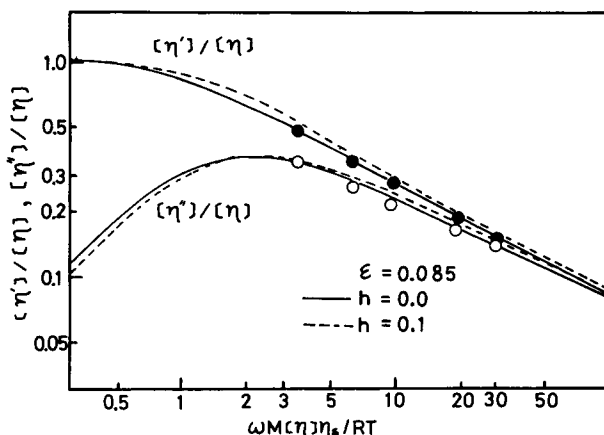


Fig. 12. Dimensionless plot of intrinsic viscosity for aqueous solution of methylcellulose at  $10^\circ\text{C}$ : (●) real part; (○) imaginary part of the complex intrinsic viscosity. Curves are drawn according to the Tschoegl theory with parameters  $\epsilon$  and  $h$  as indicated in the figure.

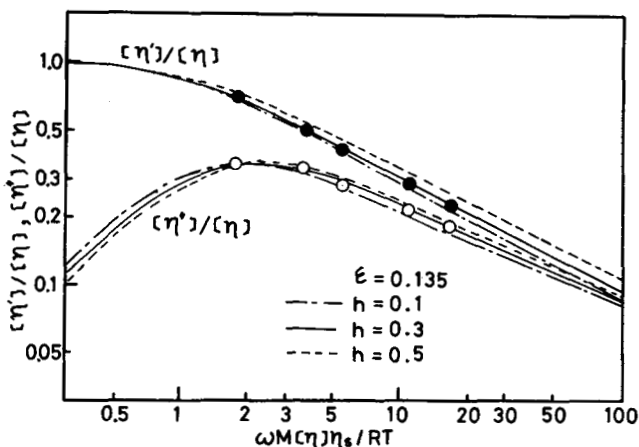


Fig. 13. Dimensionless plot of intrinsic viscosity for aqueous solution of methylcellulose at 25°C: (●) real part; (○) imaginary part of the complex intrinsic viscosity. Curves are drawn according to the Tschoegl theory with parameters  $\epsilon$  and  $h$  as indicated in the figure.

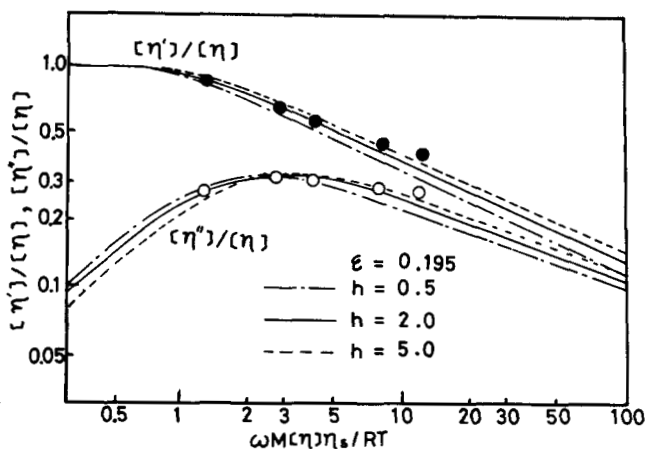


Fig. 14. Dimensionless plot of intrinsic viscosity for aqueous solution of methylcellulose at 40°C: (●) real part; (○) imaginary part of the complex intrinsic viscosity. Curves are drawn according to the Tschoegl theory with parameters  $\epsilon$  and  $h$  as indicated in the figure.

$\epsilon = 0.085$ ,  $h = 0.1$ , where  $h$  is an adjustable parameter describing the strength of hydrodynamic interaction in the Tschoegl theory. The experimental values and those frequency dependences at 10°C agree quantitatively with the Tschoegl theory with  $\epsilon = 0.085$  and  $h = 0$ , corresponding to Rouse-like behavior. In Figure 13, the experimental results at 25°C also fit the Tschoegl theory very well with  $\epsilon = 0.135$  and  $h = 0.3$ . In Figure 14, the data at 40°C are comparatively close to the theoretical

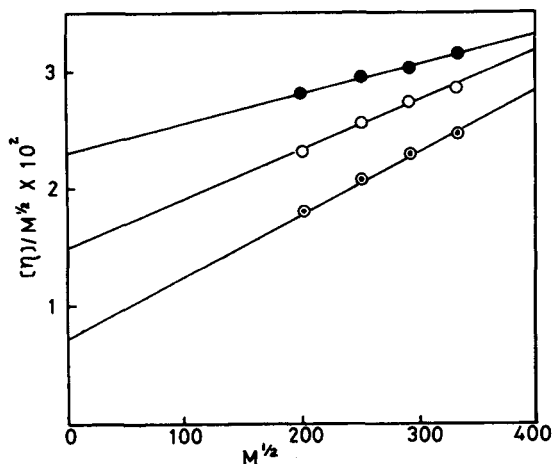


Fig. 15. Plot of  $[\eta]/M^{1/2}$  vs.  $M^{1/2}$  for methylcellulose in water: (●) measured at 10°C; (○) measured at 25°C; (⊙) measured at 40°C.

TABLE II  
Comparison of Viscoelastic Parameters

Temp., °C	$[\eta]$ , ml/g	$\epsilon$	$h$
10	845	0.085	0
25	706	0.135	0.3
40	578	0.195	2-5

curves predicted by the Tschöegl theory with  $\epsilon = 0.195$ ,  $h = 2$  or  $\epsilon = 0.195$ ,  $h = 5$ . However, there are small discrepancies between experimental values and theoretical curves, especially at high frequency range. This high-frequency behavior may be due to the influence of the intramolecular stiffness or the internal viscosity.<sup>17,18</sup>

The above-mentioned values of  $\epsilon$  and  $h$  are listed in Table II. From these results, the following conclusions may be deduced. With increasing temperature, the bonds between the polymer chains and water molecules are broken, so that methylcellulose molecules will associate or bond together, and the aggregation of methylcellulose chains occurs wherein the internal freedom and stiffness of polymer chains are affected. These phenomena cause the deviation from Gaussian chain statistics. The value of  $h$  becomes larger with increasing temperature. However, the values for an aqueous solution of methylcellulose are smaller than those for other polymers having the same order of molecular weight such as polystyrene in nonpolar solvents, even in good solvents.<sup>19</sup> Therefore, it may be deduced that the viscoelastic properties and the frequency dependence for methylcellulose in water are relatively close to Rouse-like behavior.

The authors wish to thank Dr. S. Nakamura for his useful suggestions.

## References

1. T. Amari and M. Nakamura, *J. Appl. Polym. Sci.*, **17**, 589 (1973).
2. T. Amari and M. Nakamura, *J. Appl. Polym. Sci.*, **17**, 3439 (1973).
3. W. P. Masson, *Trans. ASME*, **69**, 359 (1947).
4. W. O. Baker, W. P. Masson, and J. H. Heiss, *J. Polym. Sci.*, **8**, 129 (1953).
5. Y. Wada, H. Sasabe, and M. Tomono, *Biopolymer*, **5**, 887 (1967).
6. M. Nakamura and T. Amari, *J. Soc. Mater. Sci. Japan*, **22**, 430 (1973).
7. T. Amari and M. Nakamura, *Nippon Kagaku Kaishi (J. Chem. Soc. Japan)*, 2207 (1973).
8. P. E. Rouse and K. Sittle, *J. Appl. Phys.*, **24**, 690 (1953).
9. Y. Torikai and K. Negishi, *Oyo Butsuri*, **25**, 158 (1956).
10. N. W. Tschoegl, *J. Chem. Phys.*, **39**, 149 (1963).
11. N. W. Tschoegl, *J. Chem. Phys.*, **40**, 473 (1964).
12. A. F. Martin, paper presented at the Memphis Meeting of the American Chemical Society, April 1942.
13. H. M. Spurlin, A. F. Martin, and H. G. Tennes, *J. Polym. Sci.*, **1**, 63 (1946).
14. W. H. Stockmayer and M. Fixman, *J. Polym. Sci.*, **C1**, 137 (1963).
15. N. W. Tschoegl and J. D. Ferry, *J. Phys. Chem.*, **68**, 867 (1964).
16. J. E. Frederick, N. W. Tschoegl, and J. D. Ferry, *J. Phys. Chem.*, **68**, 1974 (1964).
17. J. D. Ferry, L. A. Holmes, J. Lamb, and A. J. Matheson, *J. Phys. Chem.*, **70**, 1685 (1966).
18. A. Peterlin, *J. Polym. Sci. A-2*, **5**, 179 (1967).
19. R. M. Johnson, J. L. Shrag, and J. D. Ferry, *Polym. J.*, **1**, 742 (1970).

Received December 27, 1973

Revised May 14, 1974